Chemical Geology 584 (2021) 120540

Contents lists available at ScienceDirect

Chemical Geology

journal homepage: www.elsevier.com/locate/chemgeo

Investigating the effect of enhanced oil recovery on the noble gas signature of casing gases and produced waters from selected California oil fields

R.L. Tyne [a,*], P.H. Barry [a,b], R. Karolytė [a], D.J. Byrne [a,c], J.T. Kulongoski [d], D.J. Hillegonds [a], C. J. Ballentine [a]

[a] Dept. of Earth Sci., University of Oxford, Oxford, UK
[b] Dept. of Marine Chem. and Geochem, Woods Hole Oceanographic Institution, Woods Hole, MA, USA
[c] CRPG-CNRS, Université de Lorraine, Nancy, France
[d] U.S. Geological Survey, California Water Science Center, San Diego, CA, USA

ARTICLE INFO

Editor: Don Porcelli

Keywords:
Noble gas isotopes
Produced fluids
Casing gas
Enhanced oil recovery
Hydrocarbon systems

ABSTRACT

In regions where water resources are scarce and in high demand, it is important to safeguard against contamination of groundwater aquifers by oil-field fluids (water, gas, oil). In this context, the geochemical characterisation of these fluids is critical so that anthropogenic contaminants can be readily identified. The first step is characterising pre-development geochemical fluid signatures (i.e., those unmodified by hydrocarbon resource development) and understanding how these signatures may have been perturbed by resource production, particularly in the context of enhanced oil recovery (EOR) techniques. Here, we present noble gas isotope data in fluids produced from oil wells in several water-stressed regions in California, USA, where EOR is prevalent. In oil-field systems, only casing gases are typically collected and measured for their noble gas compositions, even when oil and/or water phases are present, due to the relative ease of gas analyses. However, this approach relies on a number of assumptions (e.g., equilibrium between phases, water-to-oil ratio (WOR) and gas-to-oil ratio (GOR) in order to reconstruct the multiphase subsurface compositions. Here, we adopt a novel, more rigorous approach, and measure noble gases in both casing gas and produced fluid (oil-water-gas mixtures) samples from the Lost Hills, Fruitvale, North and South Belridge (San Joaquin Basin, SJB) and Orcutt (Santa Maria Basin) Oil Fields. Using this method, we are able to fully characterise the distribution of noble gases within a multiphase hydrocarbon system. We find that measured concentrations in the casing gases agree with those in the gas phase in the produced fluids and thus the two sample types can be used essentially interchangeably.

EOR signatures can readily be identified by their distinct air-derived noble gas elemental ratios (e.g., $^{20}Ne/^{36}Ar$), which are elevated compared to pre-development oil-field fluids, and conspicuously trend towards air values with respect to elemental ratios and overall concentrations. We reconstruct reservoir $^{20}Ne/^{36}Ar$ values using both casing gas and produced fluids and show that noble gas ratios in the reservoir are strongly correlated ($r^2 = 0.88–0.98$) to the amount of water injected within ~500 m of a well. We suggest that the $^{20}Ne/^{36}Ar$ increase resulting from injection is sensitive to the volume of fluid interacting with the injectate, the effective water-to-oil ratio, and the composition of the injectate. Defining both the pre-development and injection-modified hydrocarbon reservoir compositions are crucial for distinguishing the sources of hydrocarbons observed in proximal groundwaters, and for quantifying the transport mechanisms controlling this occurrence.

1. Introduction

The environmental effects of oil production, enhanced oil recovery (EOR) techniques, and hydraulic fracturing need to be understood in order to safeguard nearby water resources. EOR is the injection of surface fluids (e.g., water, steam, CO_2) into a reservoir to increase oil production by means of displacing oil or lowering its viscosity. This is similar to, but distinct from, hydraulic fracturing - the injection of water, chemicals and sand to proliferate fractures in order to promote hydrocarbon production. There is growing concern about the effects of hydrocarbon production on overlying aquifers, which are particularly valuable resources in semi-arid regions such as California (e.g., EPA,

* Corresponding author.
E-mail address: rebecca.tyne@earth.ox.ac.uk (R.L. Tyne).

https://doi.org/10.1016/j.chemgeo.2021.120540
Received 19 March 2021; Received in revised form 2 September 2021; Accepted 21 September 2021
Available online 25 September 2021

2015). The detection and quantification of oil-field fluids (oil, gas, produced fluids) within groundwater, requires an understanding of the geochemical composition of the pre-development hydrocarbon reservoir (unmodified by hydrocarbon production) and the extent to which it may have been perturbed during production.

Noble gases are powerful conservative geochemical tracers of subsurface fluids that can be used to quantify volumes of water, gas and oil contributing to a particular multiphase fluid system (e.g., Bosch and Mazor, 1988; Ballentine et al., 1991, 1996, 2002). Once incorporated into subsurface fluids, noble gases are only fractionated by physical processes, such as phase partitioning and diffusion. Terrestrial noble gas reservoirs (atmosphere, crust and mantle) have distinct isotopic compositions, which allow fluids from each reservoir to be readily differentiated. Hydrocarbon phases are initially devoid of all atmospheric noble gases and gain their unique signatures by interactions with air-saturated waters (ASW), which inherit their geochemical signature via atmospheric equilibration at recharge (e.g., Ballentine and Hall, 1999; Aeschbach-Hertig et al., 1999; Kipfer et al., 2002). This subsequent redistribution – from water to oil – is solubility controlled and is a function of the thermodynamic conditions and the relative volumes involved. Noble gases have been successfully applied as tracers in hydrocarbon systems and have provided essential information in developing our understanding of such systems (Zaikowski and Spangler, 1990; Ballentine et al., 1991; Pinti and Marty, 1995; Ballentine et al., 1996; Torgersen and Kennedy, 1999; Zhou et al., 2005; Gilfillan et al., 2008, 2009; Hunt et al., 2012; Darrah et al., 2015; Barry et al., 2016, 2017, 2018a, 2018b; Byrne et al., 2018, 2020; Scott et al., 2021). Furthermore, noble gases have also been shown to be useful tracers of thermogenic hydrocarbon gases in shallow aquifers (Darrah et al., 2014, 2015; Wen et al., 2017; Harkness et al., 2017) and for understanding the effects of EOR in hydrocarbon reservoirs (LaForce et al., 2014; Györe et al., 2015, 2017; Barry et al., 2018a). In hydrocarbon systems that have been perturbed by anthropogenic processes such as EOR and hydraulic fracturing, defining end-members for evaluating potential mixing with groundwater requires the determination of the pre-development reservoir noble gas compositions and how these signatures have evolved with production, as well as with the secondary effects of EOR.

There have been limited noble gas studies in oil dominated systems (Pinti and Marty, 1995; Ballentine et al., 1996; Torgersen and Kennedy, 1999; Györe et al., 2017; Barry et al., 2018a, 2018b) and these studies have mostly focused on casing gases, that exsolve from subsurface fluids and travel up the well annulus during production (e.g., Supplementary Fig. 1 in Tyne et al. (2019)). Subsequent phase and reservoir reconstructions have been made using gas solubility in oil and assuming 100% of the noble gases have partitioned to the gas phase. However, the measured distribution of noble gases in the different phases from the same well has not been systemically explored and thus the biases involved in the assumptions for phase and reservoir reconstructions have never been comprehensively investigated. To validate these assumptions and methods, both the casing gases (CG) and produced fluids (PF; oil-water-gas mixtures taken directly at the wellhead) must be fully characterised. The development of an extraction and purification method and more precise analyses of noble gases allow for the characterisation of all noble gas concentrations and isotope ratios in multiphase samples, such that produced fluids can now be directly analysed (Tyne et al., 2019). As a result, for the first time we are able to investigate the distribution of noble gases between casing gases and the phases that constitute produced fluids, allowing for the validity of previous assumptions to be investigated.

Specifically, this work compares noble gas distributions in casing gas and produced fluid samples from the Fruitvale, Lost Hills, North and South Belridge and Orcutt Oil Fields in California. Casing gas results from the Lost Hills Oil Field were reported in Barry et al. (2018a) and produced fluids from Fruitvale Oil Field were reported in Tyne et al. (2019). These data are used to: 1) compare the noble gas distribution within the reservoir fluids for various samples types, 2) reconstruct reservoir noble gas signatures, 3) establish pre-development reservoir noble gas signatures, 4) establish the effect of EOR injection on the noble gas distribution and 5) determine the controlling processes across multiple oil fields. These will provide a characterisation of both the pre-development and current reservoir endmembers, which are critical for distinguishing and quantifying any hydrocarbon fluids that may be present in overlying aquifers. This work is part of the California State Water Resources Control Board (SWRCB) Oil and Gas Regional Monitoring Program (RMP) to evaluate potential pathways, natural or anthropogenic, between hydrocarbon-bearing formations and groundwater resources (Taylor et al., 2014; California State Water Resources Control Board, 2020).

2. Geological context

The Fruitvale, Lost Hills and North and South Belridge Oil Fields are located in Kern Country, at the southern end of the San Joaquin Basin (SJB) in the south of the Central Valley of California. The Orcutt Oil Field is distinct from the other fields in this study, being located within the Santa Maria Basin in coastal Santa Barbara County (Fig. 1). A summary of the samples' site characteristics in each field can be found in Supplementary Table 1 and description of the oil fields can be found in the supplementary information. All these fields have been extensively injected with water, and sometimes steam, for EOR over the course of many decades. The Lost Hills, North and South Belridge, and Fruitvale Oil Fields have similarly had extensive injections for produced water disposal and pressure management. Although >90% of hydraulic fracturing in California occurs in the Lost Hills and Belridge (North and South) Oil Fields, hydraulic fracturing accounted for <0.5% of total water volume injection during 2014–17 (McMahon et al., 2018). Hydraulic fracturing has also been allegedly tested in the Orcutt Oil Field (Kanamori and Hauksson, 1992). Volumes of injection for EOR and produced water disposal are orders of magnitude larger than volumes of injection for hydraulic fracturing in these fields. No hydraulic fracturing is known to have occurred in the Fruitvale Oil Field.

3. Methods

3.1. Sample collection

During 2016, 11 casing gas and 11 produced fluid samples were collected from the Lost Hills (CG $n = 8$, PF $n = 5$), Fruitvale (PF $n = 6$) and North and South Belridge (CG $n = 3$) Oil Fields. A further six pairs of casing gas and produced fluid samples were collected from the Orcutt Oil Field in 2018. All samples were collected as part of the RMP at wells that are close to EOR injection (within 500 m) and at wells more than 500 m from injection. Sample types from each field can be found in Supplementary Table 1.

Produced fluid samples were collected in 3/8″ refrigeration-grade copper tubes with stainless steel clamps using methods previously described (Tyne et al., 2019). The copper (Cu) tubes were connected to the wellhead sampling point using reinforced PTFE tubing and hose clamps. A 'T-connection' was fitted at the wellhead to ensure the tubing did not become over pressurised once the Cu tubes were sealed. Cu tubes were flushed with produced fluids prior to sampling. Casing gases were also collected in Cu tubes using standard sampling methods using a two-stage regulator attached to the well head which stepped the pressure down to 1–2 bars (Burnard, 2013). Cu tubes were flushed with casing gases for 10 minutes minutes with the end submerged into water to prevent any backflow before being sealed with stainless steel clamps (Weiss, 1968).

3.2. Analytical techniques

Noble gas analyses were conducted in the Noble Laboratory at the University of Oxford, UK, using two noble gas mass spectrometers

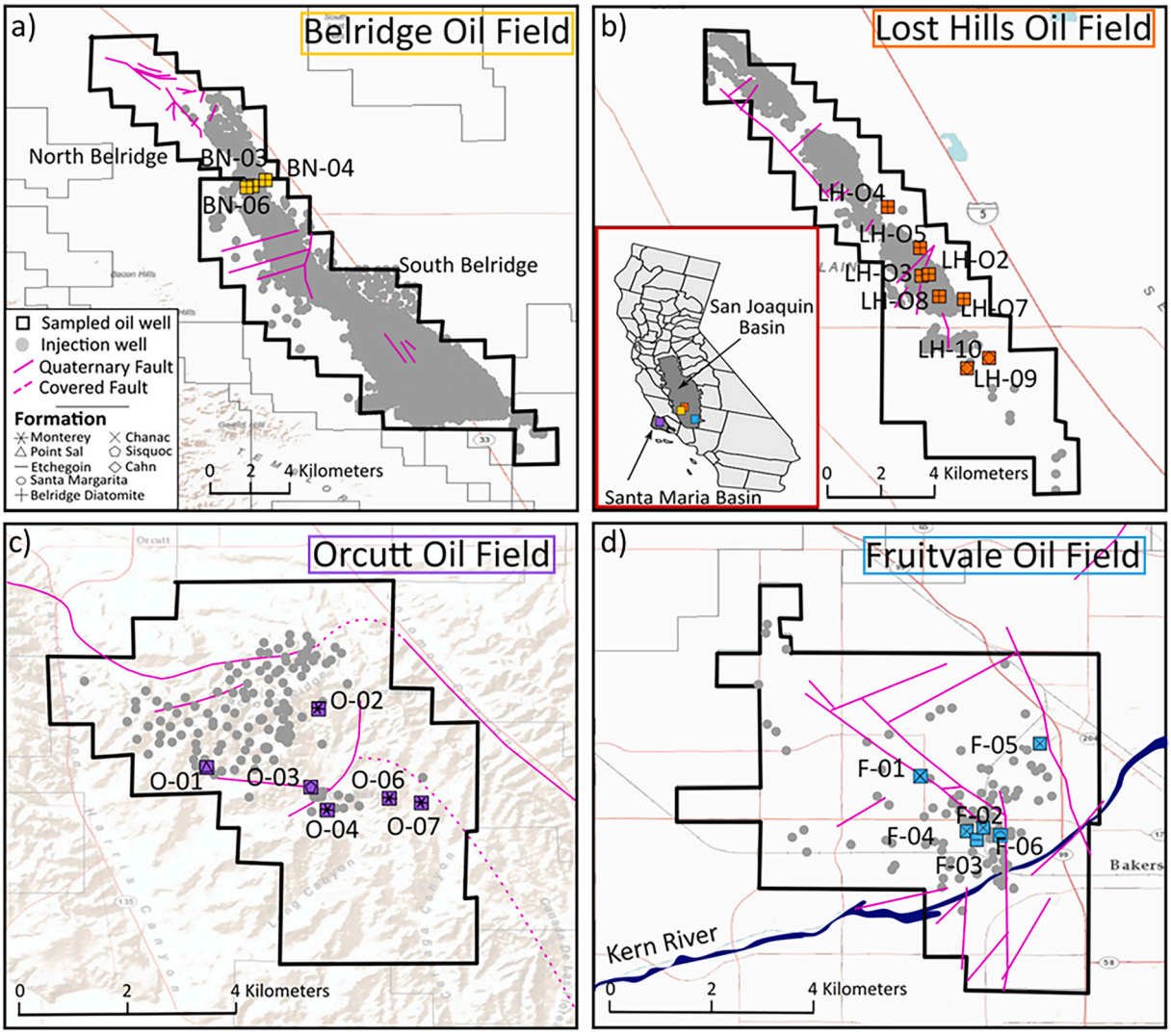

Fig. 1. Location of study oil fields and sampling sites (coloured squares)Division of Oil Gas and Geothermal Resources (DOGGR), 2017. Injection wells (grey circles) are those used for water flooding, water disposal, steam flooding, and water and cyclic steam injection (CalGEM, 2020). Producing formation is indicted by a symbol for each well; these symbols are consistent throughout the manuscript. Oil field boundaries and Quaternary and major inactive faults have been sourced from (California Geological Survery, 2021) and (USGS, 2019), respectively. Topography is from ESRI, 2020.

interfaced to a dedicated hydrocarbon extraction and purification line, as well as a dedicated offline fluid extraction system. Gases were initially extracted from the produced fluids using an offline double capillary method to quantitatively isolate noble gases into a transfer vessel, while effectively removing all water, oil, and less volatile hydrocarbons (Tyne et al., 2019). Relative volumes of gas, water and oil, as well as the full tube volume, were then recorded. The extracted gases and casing gases were then purified of their hydrocarbons and other reactive gases and analysed on a Thermo Helix SFT and Thermo Argus IV. Full procedures can be found in Barry et al. (2016, 2018a) and Tyne et al. (2019).

3.3. Calculating noble gas concentrations within produced fluids

In order to compare the noble gas concentrations in the multi-phase produced fluids and casing gases at the wellhead, the concentration of noble gas within each phase of the produced fluid need to be calculated from the measured total noble gas abundance. The abundance of noble gas *i* in the oil ($[i]_o$), gas ($[i]_g$) and water ($[i]_w$) can be calculated relative to each other at the time of sampling using their relative solubilities (parameterised by Henry's Constant for each element), production temperatures, sampling salinity and oil density (eq. (1) and (2)). Production temperatures, sample salinity and oil density can be found in Gannon et al. (2018) and Seitz et al. (2021).

$$[i]_o = \frac{[i]_g \times V_o}{K^i_{go} \times V_g} \quad (1)$$

$$[i]_w = \frac{[i]_g \times V_w}{K^i_{gw} \times V_g} \quad (2)$$

V_o, V_g and V_w are the volumes of oil, gas, and water respectively that are measured in the sample tube. K^i_{gw} and K^i_{go} are the Henry's Constants for species *i* between gas and water and gas and oil respectively. K^i_{gw} and K^i_{go} are temperature, salinity and pressure dependent and can be calculated as in Crovetto et al. (1982), Kharaka & Specht (1988) and Fernández-Prini et al. (2003). Using the total abundance of noble gases measured within the produced fluid and the relative volumes of each phase at the wellhead, the concentration in each phase can be calculated (eq. (3)–(5), Tyne et al. (2019))

$$C^i_g = \frac{[i]_m \times [i]_g \times 22400}{\left([i]_g + [i]_o + [i]_w\right) \times GOR} \quad (3)$$

$$C_o^i = \frac{[i]_m \times [i]_o \times 22400}{\left([i]_g + [i]_o + [i]_w\right)} \quad (4)$$

$$C_w^i = \frac{[i]_m \times [i]_w \times 22400}{\left([i]_g + [i]_o + [i]_w\right) \times \mathrm{WOR}} \quad (5)$$

where C_g^i, C_o^i and C_w^i are the concentration in the gas (cm^3 STP/cm^3), oil (cm^3 STP/g) and water (cm^3 STP/g) phase respectively. $[i]_m$ is the total abundance of noble gas species i measured in the sample. The variable nature of the produced fluid compositions at the wellhead means that the water-to-oil ratio (WOR) and gas-to-oil ratio (GOR) are not consistent during sampling and are not representative of the average GOR and WOR for production. Therefore, instead of using V_o, V_w and V_g to calculate the concentrations, the average time integrated GOR and WOR (Supplementary Table 1) are used. If one phase is not present within the produced fluid collected, the concentration in the missing phase can be calculated based on phase equilibrium under wellhead conditions. The calculated concentration in the gas phase can then be directly compared to that measured in the casing gas. From the concentration in the casing gases, the expected concentrations in the oil and water phase can also be calculated based on relative solubility.

4. Results

4.1. Casing gas results

Casing gases were collected from the Lost Hills, North and South Belridge and Orcutt Oil Fields; measured concentrations can be found in Supplementary Table 2 and isotope ratio data can be found in Supplementary Table 3, as well in USGS data releases (Gannon et al., 2018; Seitz et al., 2021).

Measured helium (^{4}He) concentrations in the casing gases across the sites vary from 4.8 ± 0.4 × 10^{-8} to 3.3 ± 0.1 × 10^{-5} cm^3 STP/cm^3 (where STP is standard temperature and pressure) (Fig. 2). Samples from the SJB sites (Lost Hills & North and South Belridge Oil Fields) have helium isotope ratios (^{3}He/^{4}He) relative to air ($R_A = 1.4 \times 10^6$) of 0.013 ± 0.001 to 0.06 ± 0.003 R_A, which suggests that they are dominated by radiogenic ^{4}He (where the radiogenic production ^{3}He/^{4}He value = 0.02 R_A). However, in the Orcutt Oil Field, ^{3}He/^{4}He ranges from 0.051 ± 0.001 to 0.572 ± 0.006 R_A, indicative of a mantle helium contribution (Fig. 2). Using the expected radiogenic production value and assuming a mantle helium isotopic composition of 6.1 ± 2.1 R_A (Day, et al., 2015), the Orcutt Oil Field samples show up to a 9% mantle helium contribution. The most elevated helium isotope ratios are found in samples O-01, O-02, and O-03, to the west of the active faults within the field (Fig. 1cc), suggesting that these faults are acting as a conduit for mantle derived fluids (Kulongoski et al., 2003, 2005, 2013). Fluid migration along a fault is in agreement with findings from Hummel (2009), who found that the activation and reactivation of faulting within the Orcutt Oil Field provided conduits for fluid migration.

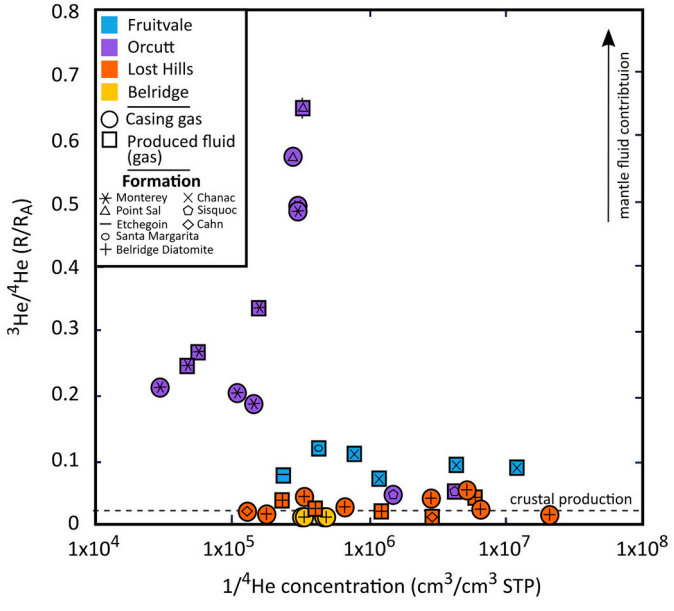

Fig. 2. Helium (^{4}He) concentrations and isotope data (^{3}He/^{4}He) in both the casing gas and gas phase of produced fluid. Helium isotopes are normalised to air (where air = 1R_A). Helium isotopes show that helium in all fields is largely radiogenic, with the exception of the Orcutt Oil Field that has more elevated helium isotopes likely due to a mantle influx from its proximity to faults (e.g. Kulongoski et al., 2013). 1σ uncertainties are less than 5% and within symbol size for most samples.

Across the three fields, neon (^{20}Ne) concentrations range from 1.85 ± 0.04 × 10^{-9} to 28.6 ± 0.4 × 10^{-9} cm^3 STP/cm^3. Measured ^{20}Ne/^{22}Ne and ^{21}Ne/^{22}Ne ratios vary between 9.38 ± 0.05 and 10.2 ± 0.1 and 0.0283 ± 0.0002 and 0.0305 ± 0.0002. Deviations from the atmospheric ^{20}Ne/^{22}Ne (9.8) and ^{21}Ne/^{22}Ne (0.0290) can be attributed to mass dependent fractionation effects.

Measured argon isotope (^{40}Ar/^{36}Ar) values are above the atmospheric value (298.56; Lee et al., 2006), with measured values between 291.8 ± 0.4 to 501.5 ± 0.6, showing a resolvable radiogenic ^{40}Ar concentration in each of the oil fields. Measured ^{38}Ar/^{36}Ar values are predominantly air-like. Argon (^{36}Ar) concentrations in the casing gases range from 10.0 ± 0.1 to 219 ± 2 × 10^{-9} cm^3 STP/cm^3.

Measured krypton and xenon isotope ratios are indistinguishable from air. Krypton (^{84}Kr) concentrations from the Lost Hills, Orcutt and North and South Belridge Oil Fields casing gases range from 1.42 ± 0.03 to 12.2 ± 0.3 × 10^{-9} cm^3 STP/cm^3. The xenon (^{130}Xe) concentrations in the three fields range from 111 ± 2 to 529 ± 11 × 10^{-12} cm^3 STP/cm^3.

4.2. Produced fluid results

Produced fluids were collected from the Fruitvale, Lost Hills and Orcutt Oil Fields. Wellhead concentrations from each phase of the produced fluids are reported in Supplementary Table 2. These have been calculated following methods described in section 3.3 and in more detail in Tyne et al. (2019). Due to solubility within elements being approximately the same for all isotopes, differences in the noble gas isotope ratios between the phases are expected to be negligible and therefore only the overall produced fluid ratio is reported (Supplementary Table 3). Within an oil-water system, higher noble gas concentrations are expected in the oil phase compared to the water phase (Ballentine et al., 1996; Tyne et al., 2019). During production, gases exsolve from the denser fluids and typically exhibit the highest noble gas concentrations of all three phases. We observe this partitioning trend within the produced fluids, where the gas phase concentrations are >2 orders of magnitude higher than oil concentrations, which contain approximately twice the amount of noble gases as the water phase (Supplementary Table 2).

The ^{4}He concentration within the exsolved gases in the produced fluid samples range from 0.084 ± 0.002 to 21.1 ± 0.6 × 10^{-6} cm^3 STP/cm^3, with the largest ^{4}He concentration range within the Orcutt Oil Field (Fig. 2). The ^{4}He concentrations calculated in the oil and water phases were significantly lower at 6.24 ± 0.23 to 37,400 ± 1100 × 10^{-15} mol/g_{oil} and 3.04 ± 0.11 to 17,000 ± 500 × 10^{-15} mol/g_{water} respectively. Similarly to the casing gases, the ^{3}He/^{4}He in the produced fluids from Lost Hills Oil Field are strongly radiogenic (0.014 ± 0.001 to 0.042 ± 0.001 R_A). Fruitvale Oil Field has a slightly less radiogenic signature (0.068 ± 0.001 to 0.17 ± 0.002 R_A), whilst Orcutt Oil Field again shows a variable mantle contribution with ^{3}He/^{4}He ranging from 0.052 ± 0.001–0.648 ± 0.08 R_A in agreement with the casing gases.

Neon (^{20}Ne) concentrations vary from 0.086 ± 0.004 to 90.6 ± 0.9 ×

10^{-9} cm^3 STP/cm^3 in the gas phase of the produced fluids. Concentrations of ^{20}Ne in the oil and water phases within the sample fields are between 0.025 ± 0.001 to 35 ± 1 × 10^{-15} mol/g_{oil} and 0.016 ± 0.001 to 7.7 ± 0.4 × 10^{-15} mol/g_{water}, respectively. $^{20}Ne/^{22}Ne$ and $^{21}Ne/^{22}Ne$ ratios within the produced fluids are in agreement with the casing gases at 9.80 ± 0.14 to 10.5 ± 0.2 and 0.0278 ± 0.0002 to 0.0310 ± 0.0002 respectively.

Fruitvale, Lost Hills and Orcutt Oil Fields ^{36}Ar concentrations in gas, oil and water phases are 4.09 ± 0.18 to 816 ± 48 × 10^{-9} cm^3 STP/cm^3, 1.02 ± 0.04 to 2500 ± 100 × 10^{-15} mol/g_{oil} and 0.218 ± 0.009 to 380 ± 20 × 10^{-15} mol/g_{water}. $^{40}Ar/^{36}Ar$ values are between 294 ± 5 and 479 ± 11 and are consistent with a radiogenic ^{40}Ar present in some samples.

Krypton isotopic ratios ($^{86}Kr/^{84}Kr$) are agreement with the air value (0.303) at 0.300 ± 0.005 to 0.309 ± 0.001 and consistent with the casing gas results. The ^{84}Kr concentrations are 0.115 ± 0.011 to 260 ± 10 × 10^{-15} mol/g_{oil} in the oil phase, 0.74 ± 0.06 to 45.1 ± 3.7 × 10^{-9} cm^3 STP/cm^3 in the gas phase and 0.102 ± 0.0008 to 28 ± 1 × 10^{-15} mol/g_{water} in the water phase.

Measured $^{132}Xe/^{130}Xe$ in the produced fluids across the fields are 6.52 ± 0.02 to 6.69 ± 0.11, consistent with both the casing gas values and air. Within the gas phase, the produced fluids had ^{130}Xe concentrations of 31.8 ± 1.5 to 2800 ± 40 cm^3 STP/cm^3 STP and 0.018 ± 0.002 to 150 ± 10 × 10^{-15} mol/g_{oil} within the oil phase. The ^{130}Xe concentrations within the water in the produced fluids were 0.018 ± 0.002 to 11 ± 2 × 10^{-15} mol/g_{water}.

5. Discussion

Casing gas and produced fluid data from the Fruitvale, Lost Hills, North and South Belridge and Orcutt Oil Fields in California are used to: 1) compare the noble gas abundance in the casing gas and gas phase of the produced fluids at the wellhead (section 5.1.), 2) reconstruct the noble gas distribution within the reservoir system for both the casing gases and produced fluids (section 5.2.), 3) characterise pristine reservoir noble gas signatures (section 5.3.), 4) quantify the effects of EOR injection on the noble gas distribution (section 5.4.), and 5) determine the controlling processes, across multiple oil fields (section 5.4.).

5.1. Comparison of casing gas and produced fluids at the wellhead

In this study, we collected both casing gases and produced fluids from the Lost Hills and Orcutt Oil Fields, which allow the distribution of noble gases between the casing gas and produced fluid (oil-water-gas) phases to be investigated for the first time. The abundances in measured casing gas samples can be directly compared to the gas phase in the produced fluids (as calculated in section 3.3.) under site-specific sampling conditions (Supplementary Table 2). By comparing the two, we are able to rigorously test the assumptions (e.g., equilibrium between phases, average WOR and average GOR) used for both the casing gas and produced fluids and determine whether these two sample types can be used interchangeably. We predict produced fluid concentrations to be more variable than casing gases due to greater systematic uncertainties associated with this sample type. For example, there are systematic uncertainties associated with how the fluids have degassed and travelled from the reservoir to the wellhead, which will be unique to each well/field, as it will depend on the production practices (e.g., pumping rate, 'shutting in' of casing gas), as well as from analytical uncertainties associated with analysing produced fluids (Tyne et al., 2019).

The produced fluids gas concentrations are within the same order of magnitude both above and below that in the casing gases. On average, measured ^{20}Ne concentrations in Lost Hills Oil Field casing gases are 2.8 ± 3.3 times higher than those exsolved from the produced fluid (Fig. 3), with two out of six samples having lower ^{20}Ne concentrations in the casing gas phase vs. the produced fluid gases. A similar variation is seen for ^{36}Ar (2.6 ± 2.6 times higher in the casing gas, Supplementary Fig. 2) at Lost Hills and in the Orcutt Oil Field (1.2 ± 1.5 and 5.5 ± 4.7 times higher in the gases within the produced fluid gases than casing gas for ^{20}Ne and ^{36}Ar respectively) (Fig. 3, Supplementary Fig. 2). This agreement between casing gas samples and gases exsolved from produced fluids at wellheads is within the expected variability from the systematic uncertainties and confirms that assumptions for both sample types are reasonable. Furthermore, the observed variability between the concentrations in two sample types does not change the overall interpretation of these data, and thus either casing gas or produced fluids can be used interchangeably to determine the noble gas composition of a reservoir. Further interrogation of these sample types using a larger dataset, which should include more well and production data, is needed to better understand the relationship between sample types and improve any associated uncertainties.

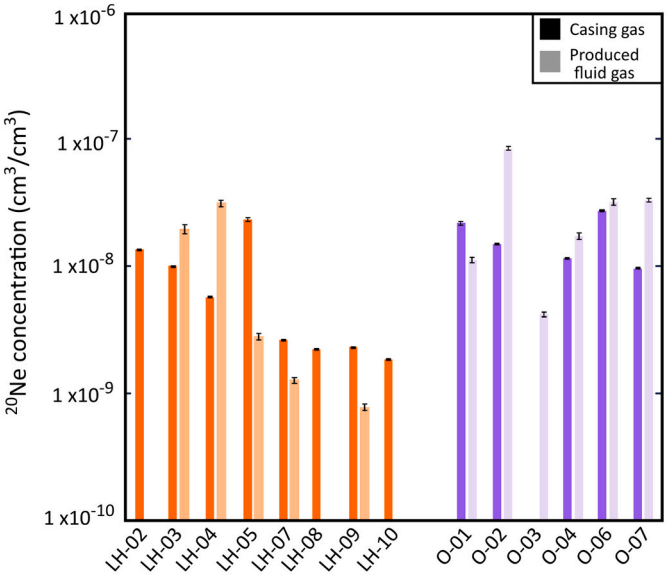

Fig. 3. Comparison of the ^{20}Ne concentration measured in the casing gases and in the gaseous phase of the produced fluid samples, where the darker bars are for the casing gas samples and lighter bars are the gaseous phase in the produced fluids. 1σ analytical uncertainties are shown. Greater variability is expected and observed in the produced fluids; however, ^{20}Ne concentrations in both sample types are in broad agreement.

5.2. Reconstructing noble gas concentrations in the reservoir oil

In hydrocarbon systems that consist predominantly of oil and water (at reservoir conditions), fluids brought to the surface during production will exsolve gases due to decompression. The noble gas content in the denser (i.e., oil and water) phases within the reservoir can be reconstructed by taking into account this exsolution during production. Previous reconstructions of the oil phase from casing gases have assumed that 100% of the gas phase is derived from the oil (Barry et al., 2018a).

However, it is probable that gases have also exsolved from the reservoir water. Here, we assume the amount of noble gases is constant between the bottom of the well and wellhead and the noble gases are distributed between the water and oil phases.

The total amount of a noble gas (n_t^i) is calculated by multiplying the calculated wellhead concentration by the relative volumes produced over a set time frame (Eq. (6)).

$$n_t^i = \frac{C_o^i \times V_o + C_g^i \times V_g + C_w^i \times V_w}{22400} \quad (6)$$

As no absolute volume measurements are available, the relative volumes are used instead (GOR and WOR). GOR and WOR are measured at the wellhead and can vary significantly over short timescales due to variation in production techniques. Here, we use the average time-

integrated GOR and WOR values (with an assumed 15% error) for each formation (Supplementary Table 1), which are likely more representative of the true values in the reservoir.

The concentration of a given noble gas, originally in the oil (C^i_{or}, mol/g_{oil}) and water (C^i_{wr}, mol/g_{water}) phases at reservoir temperature and pressure (RTP) can be estimated using eqs. (7) to (9).

$$C^i_{or} = \frac{F \times n^i_t}{V_o} \tag{7}$$

$$C^i_{wr} = \frac{F \times n^i_t}{V_w} \tag{8}$$

$$F = \frac{n^i_{or}}{n^i_{or} + \frac{V_w \times K^i_{gw} \times n^i_{or}}{V_o \times K^i_{go}}} \tag{9}$$

where F is the proportion of noble gas *i* in the oil phase. K^i_{gw} and K^i_{go} are the Henry's Constants for a given noble gas *i* under reservoir conditions. n^i_{or} is the amounts of *i* within the reservoir, as only relative proportions are needed any value can be used. Reservoir WOR is used instead of absolute volumes. Calculated oil concentrations within the reservoirs from both casing gases and produced fluids can be found in Supplementary Table 4.

5.3. Determining pre-development reservoir characteristics

In order to trace hydrocarbon contributions to shallow aquifers, it is important to first determine pre-development reservoir characteristics, as well as an understanding of how this composition has been perturbed (i.e., due to EOR) during production. As described in section 5.2, concentrations of noble gases within the oil and water in the reservoir can be reconstructed based on their solubility at depth (Supplementary Table 4.).

Atmosphere-derived noble gases (e.g., ^{20}Ne, ^{36}Ar, ^{84}Kr, ^{130}Xe) enter the subsurface dissolved in groundwater either during natural aquifer recharge or anthropogenically during injection. Krypton and xenon concentrations across all fields measured here are in excess of those predicted by solubility (Supplementary Fig. 3), as is commonly observed in hydrocarbon systems (e.g., Podosek et al., 1980; Torgersen and Kennedy, 1999; Zhou et al., 2005; Barry et al., 2016, 2018a; Wen et al., 2017; Byrne et al., 2018). This excess is likely derived from sediments but the processes controlling heavy noble gas excesses are not well-understood (Torgersen and Kennedy, 1999; Zhou et al., 2005; Barry et al., 2016). As a result, we consider only the light atmospheric gases (^{20}Ne, ^{36}Ar, which have no significant subsurface sources) in the following mixing models to evaluate the effects of injection on hydrocarbon reservoir noble gas signatures.

The solubilities of noble gases in groundwater are a function of the recharge conditions (temperature, salinity and recharge elevation, Supplementary Table 6) and generally increase with mass, allowing the initial noble gas inventory to be calculated (Ballentine and Hall, 1999; Aeschbach-Hertig et al., 1999; Kipfer et al., 2002). As oil migrates from source to the reservoir, any contact with formation waters will result in the partitioning of noble gases into the oil phase based on their relative solubility under reservoir conditions and Specific Gravity of oil (where S_g = *141.5/(API + 131.5);* Supplementary Table 1, Supplementary Table 6).

During initial charging of the reservoir (i.e., high WOR), the oil will be at its most fractionated (i.e., have the lowest ^{20}Ne/^{36}Ar, '1st bubble' composition) and as the system evolves (i.e., oil is produced) and/or more oil-water interaction occurs (WOR decreases), the ^{20}Ne/^{36}Ar$_{oil}$ will increase towards ^{20}Ne/^{36}Ar$_{ASW}$ (Fig. 4a) and concentrations of the noble gases in the oil will decrease due to dilution. Assuming a closed system equilibrium, the relative volumes of water that have exchanged with the oil can therefore be derived (Eq. (10) after Ballentine et al., 1996; Barry et al., 2016, 2018a) to predict the relative pre-development WOR within each reservoir.

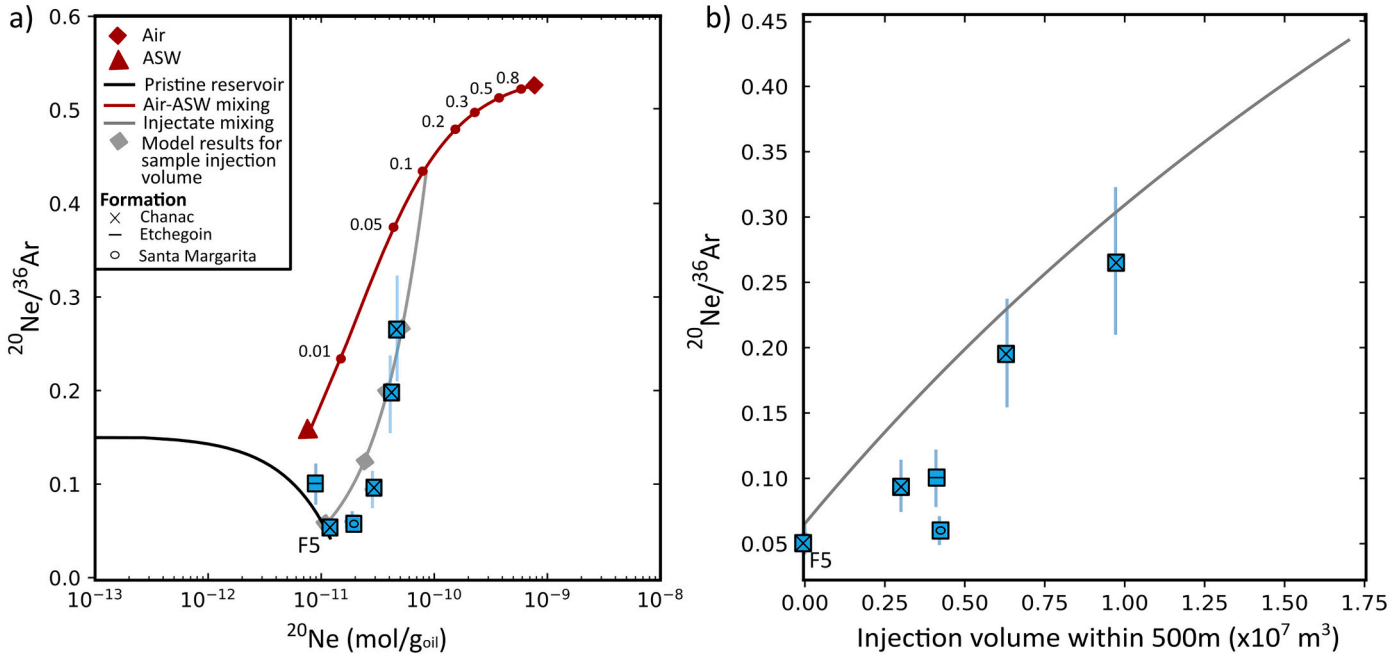

Fig. 4. Noble gas mixing models for the Fruitvale Oil Field, showing solubility partitioning and the effects of injection. a) Fruitvale Oil Field samples as a function of their ^{20}Ne/^{36}Ar vs. ^{20}Ne concentration in oil. The solid black line represents the predicted pristine hydrocarbon evolution for the reservoir conditions within the Fruitvale Oil Field and the red line represents the range of possible injectate compositions (as a function of F_{air}). Solid grey line represents the predicted mixing and reservoir evolution between the pristine reservoir and injectate using best fit V_t and F_{air} parameters (Chi-squared p = 0.15), with grey diamonds indicating model results for known sample injection volumes. Sample F5, which has seen no injection falls on the pristine reservoir evolution. b) ^{20}Ne/^{36}Ar as a function of injected water volume within 500 m. Corresponding modelled injection evolution is shown by the grey line in both panels. (For interpretation of the references to colour in this figure legend, the reader is referred to the web version of this article.)

$$WOR = \frac{[i]_{asw}}{[i]_{oil}} - \frac{K^i_{go}}{Sg \times K^i_{gw}} \quad (10)$$

where $[i]_{asw}$ is the amount of noble gas i in the formation water calculated from its recharge conditions (in mol/g) and $[i]_{oil}$ is the amount of noble gas i in the oil phase (mol/g). Henry's Constants (K^i_{go} and K^i_{gw}) were calculated under reservoir conditions (temperature, salinity and pressure) and S_g is the specific gravity of oil in g/cm^3. Sample API's can be found in Supplementary Table 1.

Assuming that the oil and water phases are in direct contact and the reservoir is in equilibrium, the pre-development concentrations of ^{20}Ne and ^{36}Ar within the hydrocarbon reservoir for different WORs can be estimated by rearranging eq. (11) (Barry et al., 2018a).

$$[i]_{oil} = \frac{[i]_{asw}}{WOR + \frac{K^i_{go}}{Sg \times K^i_{gw}}} \quad (11)$$

where $[i]_{oil}$ is calculated for each reservoir using a fixed specific gravity assumption, solubility coefficients and noble gas concentrations in the ASW (based on the unique estimated recharge conditions in each reservoir; Supplementary Table 6). The volume of injected water for each injection well within a 500 m radius of the sampled wells has been recorded and aggregated since 1977. Samples which have not been subjected to injection within 500 m display ^{20}Ne/^{36}Ar and noble gas concentrations consistent with those calculated for a pristine system (Fig. 4, Supplementary Fig. 4).

5.4. Assessing the effects of injection

During injection, noble gases are redistributed from the injected fluids into the reservoir oil, altering the pre-development composition. Samples exposed to injection within 500 m have elevated ^{20}Ne/^{36}Ar and ^{20}Ne and ^{36}Ar concentrations compared to those predicted for the pre-development reservoir (Fig. 4a, Supplementary Fig. 4), in agreement with previous findings (e.g., Barry et al., 2018a). This distinct injection signature allows us to differentiate between those samples which have been affected by EOR (i.e., have elevated ^{20}Ne/^{36}Ar, ^{20}Ne and ^{36}Ar concentrations) and pristine samples, which are characterised by equilibrium exchange (eq. (10)). These results emphasize the importance of characterising both the endmember (injectate and pre-development reservoir) composition and how this has perturbed the system over time to better distinguish the source of any hydrocarbon contributions identified in the groundwater.

Within the Lost Hills and Orcutt Oil Fields, the relationship of ^{20}Ne/^{36}Ar in reservoir oil versus injection volume for both the produced fluids and casing gases can be seen in Supplementary Fig. 5. We note that there is a similar relationship between oil values calculated from the casing gases and the produced fluids at Lost Hills Oil Field. However, at Orcutt Oil Field, elevated ^{20}Ne/^{36}Ar and ^{3}He/^{4}He in the O-02 and O-06 casing gas samples compared to the produced fluids suggests significant air contamination. Therefore, where both sample types are available, the produced fluid data appears to yield more robust results.

The calculated ^{20}Ne/^{36}Ar values in reservoir oil within the samples are strongly correlated to injected volume (within 500 m; Fig. 4b, 5). This relationship is statistically significant at a 95% confidence level in the Fruitvale, Lost Hills and North and South Belridge Oil Fields (Pearson's R correlation Fruitvale $p = 0.0032$, Lost Hills $p = 0.0030$, North and South Belridge $p = 0.0075$, Supplementary Table 5), however there is no significant relationship in the Orcutt Oil Field. This correlation implies that the noble gas composition of the reservoir during production is impacted by injection. Thus, the expected composition of a well, where other samples have been characterised, can be predicted based on its injection volume within 500 m. However, the response (i.e., increase in ^{20}Ne/^{36}Ar) to the injected water differs between oil fields, with the response in the Fruitvale Oil Field being much greater than in the other

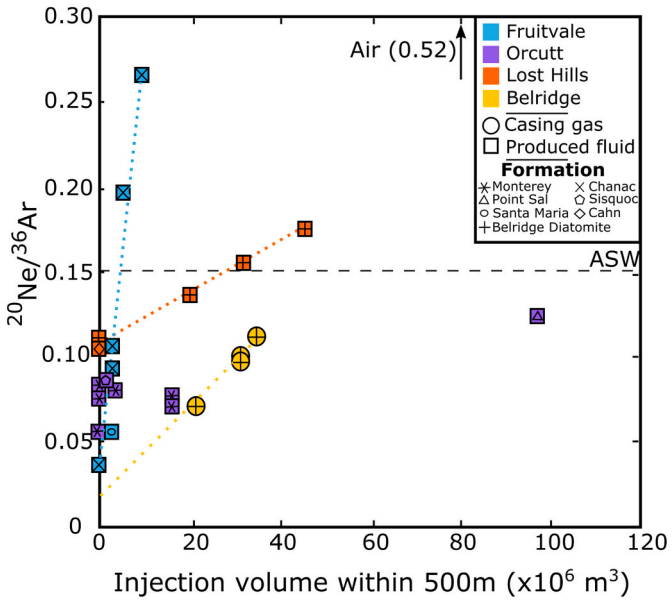

Fig. 5. Atmospheric noble gas ratio (^{20}Ne/^{36}Ar) in the reservoir oil vs. volume of injected fluids (x10^6) within 500 m of the sampled well. 1σ uncertainties encompassed by symbol sizes. There is a clear positive correlation between the injected volume and response in the atmospheric noble gas ratio (as denoted by the dashed lines), and the sensitivity of this response (increase in ^{20}Ne/^{36}Ar) appears different between the fields, with the most sensitive response (steepest slope) occurring within the Fruitvale Oil Field. Pearson's R correlation coefficients are p = 0.0032 for Fruitvale Oil Field, p = 0.0030 for Lost Hills Oil Field, p = 0.0075 for North and South Belridge Oil Fields. No significant relationship is observed within the Monterey Formation reservoir at Orcutt Oil Field.

fields (Fig. 5). We note that ^{20}Ne/^{36}Ar correlates with ^{40}Ar/^{36}Ar at the Lost Hills Oil Field but not at the Fruitvale Oil Field, perhaps due to the fact that the Lost Hills Oil Field has significantly more injection than at the Fruitvale Oil Field.

In previous studies, injected fluids have been assumed to be 'air-like' based upon measured injectate gases having elevated ^{20}Ne/^{36}Ar and elevated ^{20}Ne and ^{36}Ar concentrations (Barry et al., 2018a). However, in all sampled fields, the injected fluids are predominantly recycled produced waters and other sources, with contributions from groundwater (McMahon et al., 2018; CalGEM, 2020).

Produced waters have inherently low noble gas concentrations, as a result of stripping into the oil phase, and therefore cannot account for the elevated concentrations observed within the injected samples. We propose that during the injection process, de-oiled produced waters equilibrate with 'head space' air to reach ASW conditions, and additional entrapped air bubbles cause both the elevated concentrations and observed ratios. The injected material composition can therefore be modelled as a two-component mixture between air and ASW (Eq. 12).

$$[i]_{inj} = [i]_{ASW} \times (1 - F_{air}) + [i]_{air} \times F_{air} \quad (12)$$

where F_{air} is the fraction of air in the mixture, and $[i]_{inj}$, $[i]_{ASW}$, $[i]_{air}$ are the concentration of noble gas i in the injectate, ASW (assumed at 15 °C) and air respectively.

As there is no evidence of gas caps in the sampled fields, we assume that the injected material will mix with the oil within the reservoir and can therefore be treated as binary mixing between the pristine system oil and the injectate:

$$[i]_{res} = [i]_{pris} \times F_{pris} + [i]_{inj} \times F_{inj} \quad (13)$$

where $[i]_{inj}$, $[i]_{pris}$, $[i]_{res}$ are the concentration of noble gas i in the injectate, pristine oil and reservoir after injection. The concentration of i

in the 'pristine' oil is a function of the WOR of the system and can be calculated by rearranging eq. (10). Although we recognise that there is likely a range in pre-development reservoir compositions, we assume a common endmember, which has not been subjected to any injection (e.g., sample F5 for the Chanac reservoir at Fruitvale Oil Field), and the WOR of this sample (8.96, $^{20}Ne/^{36}Ar = 0.053$) is assumed to be representative of all pre-development WORs within the field. In fields where an unaltered sample is not available, we used the calculations to find a best-fit WOR. F_{pris} *and* F_{inj} are the fraction of pristine oil and injectate, respectively and $F_{pris} + F_{inj} = 1$. They can be calculated using the following: $F_{inj} = V_{inj}/(V_{oil} + V_{inj})$ and $F_{pris} = V_{oil}/(V_{oil} + V_{inj})$.

By iteratively calculating the effects of injection in this way for differing F_{air}, which determines the composition of injectate, and V_{oil}, we are able to determine these parameters and their associated uncertainties using non-linear least squares minimisations for each field. The minimisation is carried out using the Levenberg-Marquardt algorithm (Marquardt, 1963), and an associated Chi-Squared value is calculated. V_{oil} and F_{air} are shared parameters between samples from the same formations, while V_{inj} is the known amount of injectate, assumed to be different for each well. Within the Fruitvale Oil Field system, at 85% probability, we find that samples influenced by EOR are consistent with modelled mixtures of injectate with a best-fit fraction of air of 0.11 ± 0.04, a total volume of oil and injectate mixture of $1.7 \pm 0.7 \times 10^7$ m^3, and assuming a pristine composition of sample F5 (Fig. 4, Supplementary Table 5). This novel noble gas approach allows us to derive an estimated oil volume for which the known volume of injected fluids must have come into contact with within the reservoir. Within the Fruitvale Oil Field, this volume of oil is 2 orders of magnitude less than maximum predictions based on simple reservoir reserve estimates and size ($\sim 2 \times 10^9$ m^3; DOGGR, 1991). This difference suggests that the injected water has had restricted interaction with the reservoir fluids. A combination of the V_{oil} and F_{air} will control how the system responds to injection and how it will evolve during production.

The same model was applied to both the North and South Belridge and Lost Hills Oil Fields (Supplementary Fig. 4). For samples collected within the North and South Belridge Oil Fields, we predict that the injectates have a more 'air–like' composition than at Fruitvale Oil Field (Supplementary Fig. 4, Supplementary Table 5) and that the volume of oil exposed to the injectate (within 500 m of the well) is 2 orders of magnitude greater than at Fruitvale Oil Field, causing the smaller increase in $^{20}Ne/^{36}Ar$ with the same injected volume, (Fig. 5, Supplementary Table 5). In the Lost Hills Oil Field, the injectate fluid appears to have a larger ASW contribution and more variable pristine WOR (Supplementary Fig. 4). However, the calculated results for the North and South Belridge and Lost Hills Oil Fields were not statistically significant. It is likely that the variability within these reservoirs could be a result of: (1) differences in the injectate compositions between different injection processing tanks and injection wells; (2) differences in the ease of fluid circulation within the field (i.e., permeability and porosity), where higher permeability and porosity would increase circulation and allow for a greater volume of water per bulk unit of rock and thus, a higher effective WOR; (3) differences in migration distances, as oils with longer migration distance are likely to have been exposed to greater volumes of water; (4) compartmentalisation, whereby some stratigraphic units will have been subjected to greater volumes of water than others since flow is restricted by geological conditions and features such as faults; and (5) human induced variability as a result of production history. Notably, these explanations are not mutually exclusive and each of these will have implications on the reservoir processes. No model has been constructed for the Orcutt Oil Field due to its large degree of geo-compartmentalisation driven by Quaternary faulting across the field.

By modelling the injection within the reservoir, we are able to develop a broad reconnaissance-level understanding of the composition of the injectate and how the injectate has interacted with the pristine reservoir. As a result, the secondary overprinting of noble gas signatures by injection can be quantified, allowing for the characterisation of both the pristine reservoir and how this pristine reservoir has been perturbed and evolved with the addition of these injected fluids.

5.5. Implications for water resources

Geochemical tools provide a method for distinguishing between natural and anthropogenic sources of oil-field fluids in shallow aquifers, which is an important tool in the protection of groundwater resources. For example, noble gases can be used to distinguish between oil that is surface-derived (i.e., air-like) vs. oil that is deeply-derived (i.e., radiogenic). By characterising the distinct composition of the various components of oil field fluids (i.e., water, oil and gas phases in produced fluids or surface disposal ponds), we may be able to determine if these fluids have contacted an aquifer system, and if so, we can potentially identify fluids were involved. Here, we show that there are distinct differences in the noble gas composition of these oil field fluids, particularly in comparison to ASW. This finding demonstrates that the noble gases constitute an effective tool for identifying not only the source of any potential contamination, but also the transport within a groundwater aquifer. For example, by reconstructing noble gases originally in the fluids (under reservoir conditions), we show that oil is enriched in Kr by a factor of 14 relative to ASW and by a factor of 280 relative to ASW with respect to Xe (Supplementary Table 4). This is important, because these fluids are therefore readily identifiable due to their huge Kr and Xe excesses. Moreover, in samples heavily affected by EOR, $^{20}Ne/^{36}Ar$ is typically very high (i.e., $>>$ ASW), approaching the value of air (e.g., Fig. 5). There is also potential to use the observed excesses in radiogenic noble gases (e.g., Supplementary Table 3) as an additional constraint in any mixing model of oil-field fluids and shallow groundwater. Conversely, produced waters are stripped of their noble gases due to partitioning into the oil and gas phases, meaning they are depleted relative to ASW (up to a factor of 100 with respect to Xe) (Supplementary Table 2). Karolytė et al. (2021) applied this technique using noble gas data from the SJB oil field fluids, as well as surface disposal ponds, to identify oil-field fluid mixing in shallow aquifers and showed the clear utility of including the noble gas composition of these different endmembers when investigating potential hydrocarbon sources in groundwater.

6. Conclusions

We present noble gas data from both casing gases and produced fluids across four oil fields (Fruitvale, Lost Hills, Orcutt and North and South Belridge Oil Fields) in California, which have been subjected to variable degrees of enhanced oil recovery. Collecting both casing gas and produced fluid samples enables a comparison, for the first time, of these two samples types with regards to their noble gas concentrations. Concentrations of noble gases were on average 3.0 ± 1.8 times greater in the casing gases, validating previous methods of phase and reservoir reconstructions that rely on casing gas compositions. This validation allows for direct comparison of fields where only singular sample types are available, regardless of sample type.

We find that $^{20}Ne/^{36}Ar$ in each of the sampled fields has a strong positive correlation with the injected volume within 500 m of the sampled wells. The sensitivity of this correlation is, however, not consistent between fields, and the Fruitvale Oil Field $^{20}Ne/^{36}Ar$ values are higher as a result of injection than the Lost Hills, North and South Belridge and Orcutt Oil Fields. By developing a mixing model between the injected fluid and pristine system compositions we determine both the fraction of air injected and initial oil volume interacting with the injection fluids, which allows us to investigate how the pristine system has been perturbed during production. We conclude that the injectate composition and volume of oil are likely to be the primary controls on the magnitude of increase of $^{20}Ne/^{36}Ar$ with injection volume. This observation may help to develop a tool to quantify interaction between the injectate and reservoir fluids. However, further work is needed to

characterise the composition of the injectate fluids and the range in possible initial water-to-oil ratios within a reservoir. Understanding the composition of the pristine hydrocarbon reservoir and how it evolves with injection is critical in determining baseline endmembers for future forensic studies of groundwater quality.

Declaration of Competing Interest

The authors declare that they have no known competing financial interests or personal relationships that could have appeared to influence the work reported in this paper.

Acknowledgements

This work was supported by a Natural Environment Research Council studentship to R.L.Tyne (Grant ref. NE/L002612/1) and the U.S. Geological Survey (Grant ref. 15-080-250), as part of the California State Water Resource Control Board's Oil and Gas Regional Groundwater Monitoring Program (RMP). Data can be accessed in Supplementary Tables 1-3 and in the data release from Gannon et al. (2018) and Seitz et al. (2021). We thank the owners and operators at the Fruitvale, Lost Hills, North and South Belridge and Orcutt Oil Fields for access to wells. We also thank Matt Landon and Jennifer Harkness from the USGS who provided helpful comments on an earlier version of the manuscript.

Appendix A. Supplementary data

Supplementary data to this article can be found online at https://doi.org/10.1016/j.chemgeo.2021.120540.

References

Aeschbach-Hertig, W., Peeters, F., Beyerle, U., Kipfer, R., 1999. Interpretation of dissolved atmospheric noble gases in natural waters. Water Resour. Res. 35, 2779–2792.

Ballentine, C.J., Hall, C.M., 1999. Determining paleotemperature and other variables by using an error-weighted, nonlinear inversion of noble gas concentrations in water. Geochim. Cosmochim. Acta 63, 2315–2336.

Ballentine, C.J., O'Nions, R.K., Oxburgh, E.R., Horvath, F., Deak, J., 1991. Rare gas constraints on hydrocarbon accumulation, crustal degassing and groundwater flow in the Pannonian Basin. Earth Planet. Sci. Lett. 105, 229–246.

Ballentine, C.J., O'Nions, R.K., Coleman, M.L., 1996. A Magnus opus: Helium, neon, and argon isotopes in a North Sea oilfield. Geochim. Cosmochim. Acta 60, 831–849.

Ballentine, C.J., Burgess, R., Marty, B., 2002. Tracing Fluid Origin, Transport and Interaction in the Crust. In: Porcelli, D., Ballentine, C.J., Wieler, R. (Eds.), Noble Gases in Geochemistry and Cosmochemistry. Geochemical Society, Mineralogical Society of America, Chap, 13, pp. 539–614.

Barry, P.H., Lawson, M., Meurer, W.P., Warr, O., Mabry, J.C., Byrne, D.J., Ballentine, C. J., 2016. Noble gases solubility models of hydrocarbon charge mechanism in the Sleipner Vest gas field. Geochim. Cosmochim. Acta 194, 291–309.

Barry, P.H., Lawson, M., Meurer, W.P., Danabalan, D., Byrne, D.J., Mabry, J.C., Ballentine, C.J., 2017. Determining fluid migration and isolation times in multiphase crustal domains using noble gases. Geology 45 (9), 775–778.

Barry, P.H., Kulongoski, J.T., Tyne, R.L., Landon, M.K., Gillespie, J.M., Stephens, M.J., Hillegonds, D.J., Byrne, D.J., Ballentine, C.J., 2018a. Tracing enhanced oil recovery signatures in casing gases from the lost Hills oil field using noble gases. Earth Planet. Sci. Lett. 496, 57–67.

Barry, P.H., Lawson, M., Meurer, W.P., Cheng, A., Ballentine, C.J., 2018b. Noble gases in Deepwater oils of the U.S. Gulf of Mexico. Geochem. Geophys. Geosyst. 19, 4218–4235.

Bosch, A., Mazor, E., 1988. Natural gas association with water and oil as depicted by atmospheric noble gases: case studies from the southeastern Mediterranean Coastal Plain. Earth Planet. Sci. Lett. 87, 338–346.

Burnard, P., 2013. The Noble Gases as Geochemical Tracers. Springer.

Byrne, D.J., Barry, P.H., Lawson, M., Ballentine, C.J., 2018. Determining gas expulsion vs retention during hydrocarbon generation in the Eagle Ford Shale using noble gases. Geochim. Cosmochim. Acta 241, 240–254.

Byrne, D.J., Barry, P.H., Lawson, M., Ballentine, C.J., 2020. The use of noble gas isotopes to constrain subsurface fluid flow and hydrocarbon migration in the East Texas Basin. Geochim. Cosmochim. Acta 268, 186–208.

CalGEM, 2020. *Online Production and Injection Data.*, California Department of Conservation. CalGEM publication. Available at. ftp://ftp.consrv.ca.gov/pub/oil/Online_Data/Production_Injection_Data.

California Geological Survery, 2021. Geological Map of California. California Geoligcal Survery, California Department of Conservation. Accessed on: 11 Jan 2021, Avaliable at: https://maps.conservation.ca.gov/cgs/gmc/.

California State Water Resources Control Board, 2020. Water Quality in Areas of Oil and Gas Production – Regional Groundwater Monitoring. California State Water Resources Control Board Web Page. accessed December 7, 2020, at. https://www.waterboards.ca.gov/water_issues/programs/groundwater/sb4/regional_monitoring/.

Crovetto, R., Fernández-Prini, R., Japas, M.L., 1982. Solubilities of inert gases and methane in H_2O and in D_2O in the temperature range of 300 to 600 K. J. Chem. Phys. 76, 1077–1086.

Darrah, T.H., Vengosh, A., Jackson, R.B., Warner, N.R., Poreda, R.J., 2014. Noble gases identify the mechanisms of fugitive gas contamination in drinking-water wells overlying the Marcellus and Barnett Shales. Proc. Natl. Acad. Sci. 111, 14076–14081.

Darrah, T.H., Jackson, R.B., Vengosh, A., Warner, N.R., Whyte, C.J., Walsh, T.B., Kondash, A.J., Poreda, R.J., 2015. The evolution of Devonian hydrocarbon gases in shallow aquifers of the northern Appalachian Basin: Insights from integrating noble gas and hydrocarbon geochemistry. Geochim. Cosmochim. Acta 170, 321–355.

Day, J.M.D, Barry, P.H., Hilton, D.R., Burgess, R., Pearson, D.G., Taylor, L.A., 2015. The helium flux from the continents and ubiquity of low-3He/4He recycled crust and lithosphere. Geochimica et Cosmochimica Acta. 153, 116–133. https://doi.org/10.1016/j.gca.2015.01.008.

Division of Oil Gas and Geothermal Resources (DOGGR), 2017. GIS Mapping, DOGGR, Sacramento, CA. http://www.conservation.ca.gov/dog/maps/Pages/GISMapping2.aspx (Accessed online May 2017).

DOGGR, 1991. California Oil and Gas Fields. DOGGR publication, California Department of Conservation.

EPA, 2015. Assessment of the potential Impacts of Hydraulic Fracturing for Oil and Gas Drinking Water Resources. External Review Draft. EPA/600/R-15/047, June 2015.

ESRI, 2020. World Topographic map [Accessed 15 October 2019]. https://www.arcgis.com/home/item.html?id=30e5fe3149c34df1ba922e6f5bbf808f.

Fernández-prini, R., Alvarez, J.L., Harvey, A.H., Ferna, R., 2003. Henry 's Constants and Vapor – liquid distribution Constants for Gaseous Solutes in H_2O and D_2O at High Temperatures Henry's Constants and Vapor. J. Phys. Chem. Ref. Data 32, 903–916.

Gannon, R.S., Saraceno, J.F., Kulongoski, J.T., Teunis, J.A., Barry, P.H., Tyne, R.L., Kraus, T.E.C., Hansen, A.M., Qi, S.L., 2018. Produced Water Chemistry Data for the Lost Hills, Fruitvale, and North and South Belridge Study Areas. U.S. Geological Survey data release, Southern San Joaquin Valley, California. https://doi.org/10.5066/F7X929H9.

Gilfillan, S.M.V., Ballentine, C.J., Holland, G., Blagburn, D., Lollar, B.S., Stevens, S., Schoell, M., Cassidy, M., 2008. The noble gas geochemistry of natural CO2 gas reservoirs from the Colorado Plateau and Rocky Mountain provinces, USA. Geochim. Cosmochim. Acta 72, 1174–1198.

Gilfillan, S.M.V., Lollar, B.S., Holland, G., Blagburn, D., Stevens, S., Schoell, M., Cassidy, M., Ding, Z., Zhou, Z., Lacrampe-Couloume, G., Ballentine, C.J., 2009. Solubility trapping in formation water as dominant CO2 sink in natural gas fields. Nature 458, 614–618.

Györe, D., Stuart, F.M., Gilfillan, S.M.V., Waldron, S., 2015. Tracing injected CO2 in the Cranfield enhanced oil recovery field (MS, USA) using he, Ne and Ar isotopes. International Journal of Greenhouse Gas Control 42, 554–561.

Györe, D., Gilfillan, S.M.V., Stuart, F.M., 2017. Tracking the interaction between injected CO2 and reservoir fluids using noble gas isotopes in an analogue of large-scale carbon capture and storage. Appl. Geochem. 78, 116–128.

Harkness, J.S., Darrah, T.H., Warner, N.R., Whyte, C.J., Moore, M.T., Millot, R., Kloppmann, W., Jackson, R.B., Vengosh, A., 2017. The geochemistry of naturally occurring methane and saline groundwater in an area of unconventional shale gas development. Geochim. Cosmochim. Acta 208, 302–334.

Hummel, 2009. The Orcutt Oil Field: How stratigraphic Relationships Reflect the Structural and Tectonic History. AAPG Search and Discovery attivel (9088). Pacific Section Meeting, Ventura, California. May 3–5. http://www.searchanddiscovery.com/abstracts/html/2009/pacific/abstracts/hummel.htm.

Hunt, A.G., Darrah, T.H., Poreda, R.J., 2012. Determining the source and genetic fingerprint of natural gases using noble gas geochemistry: a northern Appalachian Basin case study. AAPG Bull. 96, 1785–1811.

Kanamori, H, Hauksson, E., 1992. A slow earthquake in the Santa Maria Basin, Cafifornia. Bullet. Seismol. Soc. Am. 82 (5), 2087–2096.

Karolytė, R., Barry, P.H., Hunt, A.G., Kulongoski, J.T., Tyne, R.L., Davis, T.A., Wright, M. T., McMahon, P.B., Ballentine, C.J., 2021. Noble Gas Constraints on the Mechanisms of Hydrocarbon Excursion into Shallow Aquifers in the San Joaquin Basin. USA, Chemical Geology.

Kharaka, Y.K., Specht, D.J., 1988. The solubility of noble gases in crude oil at 25-100 °C. Appl. Geochem. 3, 137–144.

Kipfer, R., Aeschbach-Hertig, W., Peeters, F., Stute, M., 2002. Noble Gases in Lakes and Groundwaters. In Noble Gases in Geochemistry and Cosmochemistry Geochemical Society, Mineralocical Society of Amreica, Washington DC, pp. 615–700.

Kulongoski, J.T., Hilton, D.R., Izbicki, J.A., 2003. Helium isotope studies in the Mojave Desert, California: implications for ground-water chronology and regional seismicity. Chem. Geol. 202 (1–2), 95–113.

Kulongoski, J.T., Hilton, D.R., Izbicki, J.A., 2005. Source and movement of helium in the eastern Morongo groundwater Basin: the influence of regional tectonics on crustal and mantle helium fluxes. Geochim. Cosmochim. Acta 69 (15), 3857–3872.

Kulongoski, J.T., Hilton, D.R., Barry, P.H., Esser, B.K., Hillegonds, D., Belitz, K., 2013. Volatile fluxes through the big Bend section of the San Andreas Fault, California: Helium and carbon-dioxide systematics. Chem. Geol. 339, 92–102.

LaForce, T., Ennis-King, J., Boreham, C., Paterson, L., 2014. Residual CO2 saturation estimate using noble gas tracers in a single-well field test: the CO2CRC Otway project. International Journal of Greenhouse Gas Control 26, 9–21.

Lee, J.-Y., Marti, K., Severinghaus, J.P., Kawamura, K., Yoo, H.-S., Lee, J.B., Kim, J.S., 2006. A redetermination of the isotopic abundances of atmospheric Ar. Geochim. Cosmochim. Acta 70, 4507–4512.
Marquardt, D.W., 1963. An Algorithm for Least-Squares Estimation of Nonlinear Parameters. J. Soc. Ind. Appl. Math. 11, 431–441.
McMahon, P.B., Kulongoski, J.T., Vengosh, A., Cozzarelli, I.M., Landon, M.K., Kharaka, Y.K., Gillespie, J.M., Davis, T.A., 2018. Regional patterns in the geochemistry of oil-field water, southern San Joaquin Valley, California, USA. Appl. Geochem. 98, 127–140.
Pinti, D.L., Marty, B., 1995. Noble gases in crude oils from the Paris Basin, France: Implications for the origin of fluids and constraints on oil-water-gas interactions. Geochim. Cosmochim. Acta 59, 3389–3404.
Podosek, F.A., Honda, M., Ozima, M., 1980. Sedimentary noble gases. Geochim. Cosmochim. Acta 44, 1875–1884.
Scott, J.A., Pujol, M., Györe, D., Stuart, F.M., Gilfillan, S.M.V., 2021. Determining static reservoir connectivity using noble gases. Chem. Geol. 582 (120410).
Seitz, N.O., Kulongoski, J.T., Marcusa, J.A., Qi, S.L., 2021. Produced Water Chemistry Data Collected from the Orcutt Oil Field, 2018. U.S. Geological Survey, Santa Barbara County, California. https://doi.org/10.5066/P936ZEZW.
Taylor, K.A., Fram, M.S., Landon, M.K., Kulongoski, J.T., Faunt, C.C., 2014. Oil, Gas, and Groundwater Quality in California—a discussion of issues relevant to monitoring the effects of well stimulation at regional scales.
Torgersen, T., Kennedy, B.M., 1999. Air-Xe enrichments in Elk Hills oil field gases: role of water in migration and storage. Earth Planet. Sci. Lett. 167, 239–253.
Tyne, R.L., Barry, P.H., Hillegonds, D.J., Hunt, A.G., Kulongoski, J.T., Stephens, M.J., Byrne, D.J., Ballentine, C.J., 2019. A Novel Method for the Extraction, Purification, and Characterization of Noble gases in Produced Fluids. Geochem. Geophys. Geosyst. 20, 5588–5597.
USGS, 2019. Active quaternary faults, California [Accessed 15 Oct, 2019] Available at: https://www.usgs.gov/natural-hazards/earthquake-hazards/faults?qt-science_support_page_related_con=4#qt-science_support_page_related_con.
Weiss, R.F., 1968. Piggyback sampler for dissolved gas studies on sealed water samples. Deep-Sea Res. Oceanogr. Abstr. 15 (6), 695–699.
Wen, T., Castro, M.C., Nicot, J.-P., Hall, C.M., Pinti, D.L., Mickler, P., Darvari, R., Larson, T., 2017. Characterizing the Noble Gas Isotopic Composition of the Barnett Shale and Strawn Group and Constraining the source of Stray Gas in the Trinity Aquifer, North-Central Texas. Environ. Sci. Technol. 51, 6533–6541.
Zaikowski, A., Spangler, R.R., 1990. Noble gas and methane partitioning from ground water: an aid to natural gas exploration and reservoir evaluation. Geology 18, 72.
Zhou, Z., Ballentine, C.J., Kipfer, R., Schoell, M., Thibodeaux, S., 2005. Noble gas tracing of groundwater/coalbed methane interaction in the San Juan Basin, USA. Geochim. Cosmochim. Acta 69, 5413–5428.